

Title: Tree species diversity drives the land surface phenology of seasonally dry tropical woodlands

Authors: Godlee J. L.¹, Ryan C. M.¹, Siampale A.², Dexter K. G.^{1,3}

¹School of GeoSciences, University of Edinburgh, Edinburgh, EH9 3FF, United Kingdom

²Forestry Department Headquarters - Ministry of Lands and Natural Resources, Cairo Road, Lusaka, Zambia

³Royal Botanic Garden Edinburgh, Edinburgh, EH3 5LR, United Kingdom

Corresponding author:

John L. Godlee

johngodlee@gmail.com

School of GeoSciences, University of Edinburgh, Edinburgh, United Kingdom

Acknowledgements

JLG was supported by a NERC E3 Doctoral Training Partnership PhD studentship at the University of Edinburgh (NE/L002558/1). JLG, CMR and KGD were supported by the NERC-funded SECO project (NE/T01279X/1) and the NERC-funded PhenoChange project (NE/X002993/1). All authors were supported by SEOSAW (The Socio-Ecological Observatory for Studying African Woodlands, <https://seosaw.github.io>), an activity of the Miombo Network and a NERC-funded project (NE/P008755/1).

Author contribution statement

JLG conceived the study, conducted the analysis, and wrote the first draft of the manuscript. AS coordinated field data collection in Zambia. All authors contributed to manuscript revisions.

Data accessibility statement

Field data used in this study are from the Zambian Integrated Land Use Assessment (ILUA-II). Data were cleaned and archived by the SEOSAW project (The Socio-Ecological Observatory for Studying African Woodlands). An anonymised version of the field data are available at the following DOI: <https://doi.org/10.7488/ds/7735>. Code developed for data analysis can be found here: https://github.com/johngodlee/zambia_phenology.

Abstract

1. Seasonal foliage display (leaf phenology) is a key determinant of ecosystem function. Variation in land surface phenology, observed via space-borne remote sensing, can be explained at broad spatial scales by climate, but we lack understanding of how vegetation structure and floristic diversity mediates these relationships. This lack of understanding hampers our ability to predict changes in phenology and therefore ecosystem function, in light of rapid ongoing shifts in biodiversity and ecosystem structure due to land use and climate change.
2. We combined a network of 619 vegetation monitoring sites across seasonally dry tropical deciduous woodlands in Zambia with land surface phenology metrics to investigate the role of tree species diversity, composition and vegetation structure on patterns of land surface phenology, including the phenomenon of pre-rain green-up.
3. Tree species diversity was associated with earlier pre-rain green-up, a longer growing season, and greater cumulative foliage production. Independent of diversity, proportional abundance of Detarioideae species (subfamily of Fabaceae) was associated with a longer growing season by facilitating earlier pre-rain green-up. Woodland stands with larger trees green up earlier, suggesting access to deep groundwater reserves. Senescence metrics showed variation among sites, but were not well explained by precipitation, temperature, structure or diversity.
4. **Synthesis:** Tree diversity, composition and structure are co-determinants of seasonal patterns of foliage display in seasonally dry tropical deciduous woodlands, as measured via land surface phenology, at regional scale. Our study identifies both a niche complementarity effect whereby diverse woodlands exhibit longer growing seasons, as well as a mass-ratio effect whereby detarioid species drive earlier pre-rain green-up, providing insights into the mechanisms underlying the biodiversity ecosystem function relationship in this biome. We stress the importance of considering biotic controls on ecosystem functioning in the next generation of earth-system models predicting the response of communities to global change.

1 Introduction

Foliage forms the primary interface between the vegetated land surface, the atmosphere and incoming solar radiation (Gu et al., 2003; Penuelas et al., 2009). Seasonal cycles of foliage production (leaf phenology) play an important role in regulating global carbon, water and nitrogen cycles (Garonna et al., 2016). Vegetation indices derived from remote sensing data, used as a proxy for foliage display (land surface phenology), have been used to constrain estimates of primary productivity in terrestrial biosphere models (Bloom et al., 2016; Helman, 2018), and to characterise the functional response of vegetation to various climate drivers (Richardson et al., 2013). Previous studies have identified environmental drivers of land surface phenology (Adole et al., 2019; Guan et al., 2014), but we lack understanding of how the floristic diversity and structure of the vegetation itself mediates these relationships (Whitley et al., 2017; Pau et al., 2011).

At continental scale, patterns of land surface phenology can be explained adequately using only climatic factors, namely precipitation, diurnal temperature oscillation, and photoperiod (Adole et al., 2018b; Adole et al., 2019; Guan et al., 2014), but significant local variation exists within biomes in the timing of foliage display that cannot be attributed solely to abiotic environment (Stöckli et al., 2011). Additionally, we lack a mechanistic understanding of the biotic controls on land surface phenology, which hampers our ability to make informed predictions of change in phenology under global environmental change. It has been repeatedly suggested that the diversity, composition, and structure of plant communities plays a role in determining ecosystem response to abiotic cues driving patterns of land surface phenology (Adole et al., 2018a; Jeganathan et al., 2014; Fuller, 1999), owing to differences in phenological strategy among species, but studies on this are lacking (Ma et al., 2022). Indeed, ground observations find wide variation in temporal patterns of foliage display among plant communities within a given biome (Seyednasrollah et al., 2019), but this variation is rarely represented in predictive models of biosphere-atmosphere exchanges (Scheiter et al., 2013; Pavlick et al., 2013).

Across the miombo woodlands of southern Africa, the largest woodland formation in the region (White, 1983), seasonal oscillations in water availability drive strong seasonal cycles of foliage display (Chidumayo, 2001; Dahlin et al., 2016). Within miombo woodlands, the phenomenon of pre-rain green-up, where trees produce leaves in advance of seasonal rains, serves as a striking example of phenological response to seasonal rainfall patterns. While pre-rain green-up requires heavy investment in hydraulic architecture to access deep groundwater and to produce embolism resistant hydraulic systems, it may provide competitive benefits, allowing immediate access to early rainfall and the associated release of soil nutrients prior to grass flushing (Ryan et al., 2017; February & Higgins, 2016). Detarioid species, slower growing with robust leaves, dense wood, and deep root

60 systems (Zhou et al., 2020; Timberlake & Calvert, 1993), frequently green-up before the rainy sea-
61 son has commenced. They may also retain their leaves for longer after the end of the rainy season,
62 though the mechanisms of this behaviour are unclear (Giraldo & Holbrook, 2011; Kushwaha et al.,
63 2011). Other species may only begin to produce foliage during the rainy season, creating a dense
64 flush of low cost leaves during the mid-season peak of growth and dropping their leaves earlier as
65 soil water content drops towards the end of the rainy season (Lasky et al., 2016). While species that
66 green-up early gain a competitive advantage from having fully emerged leaves once the rainy season
67 starts, they may be forced to prematurely drop their leaves to avoid excess water loss and maintain
68 a positive carbon balance if seasonal rains occur much later than normal (Vinya et al., 2018), an
69 occurrence which is becoming more common (Wainwright et al., 2021). It has been suggested that
70 variation in phenological strategy among tree species is one mechanism by which increased species
71 diversity increases resilience to, and maximises productivity in, water-limited woodland ecosystems
72 (Stan & Sanchez-Azofeifa, 2019; Morellato et al., 2016).

73 Variation in seasonal patterns of foliage display affects broader ecosystem processes. Woodlands with
74 a longer period of foliage display support a greater diversity and abundance of wildlife, particularly
75 birds, but also browsing mammals and invertebrates (Cole et al., 2015; de Araujo et al., 2017;
76 Morellato et al., 2016; Ogutu et al., 2013). As climate change reduces rainy season length and
77 increases the intensity of drought events in African water-limited woodlands (Cook et al., 2020; Gore
78 et al., 2019), woodlands with a diverse tree community may provide refugia for many animal species
79 (Bale et al., 2002). The period of green-up is a key time for invertebrate reproduction (Prather
80 et al., 2012) and herbivore browsing activity (Velasque & Del-Claro, 2016; Morellato et al., 2016).
81 Pre-rain green-up provides a valuable source of moisture and nutrients for browsing herbivores
82 before the rainy season (Makhado et al., 2018), and can moderate the understorey microclimate,
83 increasing humidity, reducing UV exposure, moderating diurnal oscillations in temperature, and
84 reducing ecophysiological stress which otherwise can lead to increased plant mortality during the
85 dry season. Thus, understanding what drives variation in seasonal patterns of foliage display in
86 tropical deciduous woodlands can provide valuable information on their vulnerability to climate
87 change, and therefore better information to predict their future composition, extent and function.

88 In this study we investigate how tree species diversity and structure influence land surface phenology
89 in seasonally dry tropical woodlands. We focus specifically on the lag between green-up/senescence
90 and the onset/end of the rainy season, the magnitude of foliage display within the growing season,
91 and the overall length of the growing season. We hypothesise that: (H_1) sites with greater species
92 diversity will exhibit a longer growing season due to a higher diversity of phenological strategies;
93 (H_2) in sites with greater species diversity the start of the growing season will occur earlier with
94 respect to the onset of the rainy season due to an increased likelihood of containing species which

95 can green-up early; (H₃) sites with larger trees will have a longer growing season, as large trees
96 can better access deep groundwater reserves outside of the rainy season; (H₄) sites dominated by
97 detarioid species will experience earlier pre-rain green-up.

98 2 Materials and methods

99 2.1 Plot data

100 We used data on tree species diversity and composition from 619 sites surveyed as part of the
101 Zambian Integrated Land Use Assessment Phase II (ILUA-II), conducted in 2014 (Mukosha &
102 Siampale, 2009; Pelletier et al., 2018). Each site consisted of four 50×20 m (0.1 ha) plots positioned
103 in a 500×500 m square around a central point (Figure 1), resulting in a total plot area per site
104 of 4000 m². The original assessment contained 993 sites, which was filtered in order to define
105 study bounds and to ensure data quality. Only sites with ≥ 50 stems ha⁻¹ ≥ 10 cm DBH (Diameter
106 at Breast Height) were included in the analysis, to ensure all sites represented woodlands with
107 a relatively continuous canopy rather than open ‘grassy savanna’, which is considered a separate
108 biome with different species composition and ecosystem processes governing phenology (Morellato
109 et al., 2013; Keith et al., 2020).

110 Plots in the ILUA-II dataset sampled stems ≥ 10 cm DBH across the area of the whole plot, while
111 stems < 10 cm DBH were only measured within a 20×10 m (0.02 ha) nested subplot. We chose to
112 use only stem measurements ≥ 10 cm DBH in this study, discarding measurements from the nested
113 subplots. In woodland ecosystems with a relatively continuous canopy like those studied here, only
114 the larger trees form the overstorey layer, with smaller trees existing within the understorey layer
115 (Chidumayo, 2001). The signal from remotely-sensed measurements of land surface phenology is
116 dominated by these larger trees which form the woodland canopy. We therefore reasoned that small
117 stems would not be an important factor in determining measurements of land surface phenology.
118 To further demonstrate the dominance of larger stems in our sites, we compared the per hectare
119 basal area contribution of stems ≥ 10 cm with that of stems < 10 cm DBH. We found that across
120 all sites, the minimum proportional basal area contributed by stems ≥ 10 cm was 72%, while the
121 median was 98%.

122 Sites with non-native tree species, e.g. *Pinus* spp. and *Eucalyptus* spp. were excluded, as these
123 species may exhibit patterns of foliage display which differ markedly from that of native tree species
124 assemblages (Broadhead et al., 2003). Of the 49 656 trees recorded, 97.9% were identified to species.
125 Sites with $> 20\%$ of trees not identified to species were discarded.

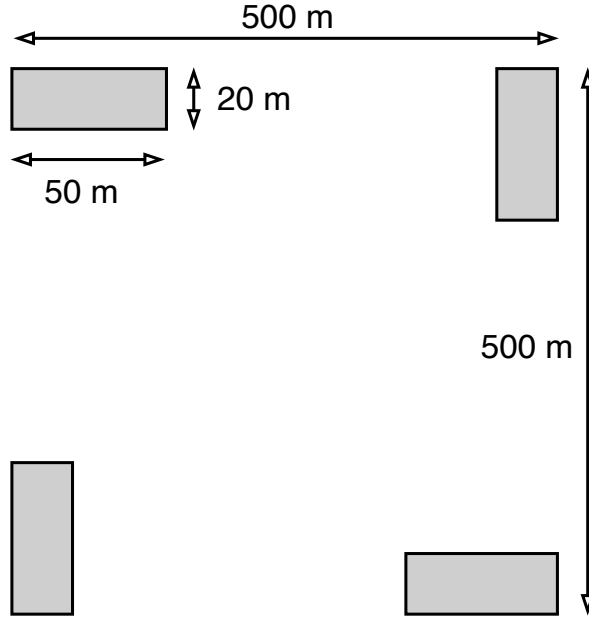


Figure 1: Schematic diagram of plot layout within a site. Each 50×20 m (0.1 ha) plot is shaded grey. Note that the plot dimensions are not to scale.

Within each plot, the species and basal area of all trees with at least one stem ≥ 10 cm DBH were recorded. Plot data were aggregated to the site level for all analyses to avoid pseudo-replication. Each site spans an area 500×500 m (0.25 km²), matching that of the land surface phenology data. We excluded sites where plots differed appreciably in vegetation composition, to ensure that all sites used in statistical analysis were representative of the vegetation within the total 0.25 km² area of each site. Using the Bray-Curtis dissimilarity index on species basal area data (Faith et al., 1987), we calculated the mean pairwise compositional distance between plots within each site. Sites were discarded when the mean pairwise compositional distance among plots within the site was greater than the mean pairwise compositional distance of all plots across all sites. This resulted in a final dataset of 619 sites.

2.2 Vegetation composition and diversity

To describe variation in tree species composition across sites we used agglomerative hierarchical clustering on species basal area data (Kreft & Jetz, 2010; Fayolle et al., 2014) to assign sites to vegetation types. We excluded species with fewer than five records across all sites from this analysis, as very rare species can hinder meaningful cluster delineation. We used Ward’s algorithm to define clusters (Murtagh & Legendre, 2014), based on the Bray-Curtis distance between pairs of sites. We determined the optimal number of clusters by maximising the mean silhouette width among clusters (Rousseeuw, 1987). We described the vegetation types represented by each cluster using

144 Dufrêne-Legendre indicator species analysis (Dufrêne & Legendre, 1997), which ranks species as the
 145 product of their relative frequency and their relative average abundance in each vegetation type.
 146 Four vegetation types were identified during hierarchical clustering. The mean silhouette value of
 147 the clustering algorithm was 0.64.

148 There was some spatial and climatic stratification in vegetation composition (Figure 2). Three
 149 miombo woodland types were identified, each with different sets of secondary species, but all dom-
 150 inated by detarioid species such as *Brachystegia* spp. and *Julbernardia* spp. (Table 1). Uapaca
 151 miombo is largely absent from the southwest of the country, occurring predominantly in higher
 152 rainfall regions to the north and east (Figure 3). *Cryptosepalum* miombo is found more in the
 153 southwest of the country, possibly representing the drier “Angolan miombo woodlands” described
 154 by White (1983). While *Cryptosepalum* miombo woodlands include *Cryptosepalum exfoliatum* as a
 155 secondary species, they should not be confused with Zambezian evergreen forests, which are domin-
 156 ated by *Cryptosepalum* (White, 1983). *Julbernardia* miombo is common in cooler areas and is more
 157 climatically restricted than the other miombo woodland types. Combretaceae woodlands match the
 158 description of small stature Zambezian woodlands, as described by Dinerstein et al. (2017) and
 159 Chidumayo (2001). These woodlands are not dominated by the same archetypal detarioid tree spe-
 160 cies as the other miombo woodland vegetation types. Combretaceae woodlands occur over a wide
 161 climatic range, and contain some of the warmest sites in our dataset in the southeast of the country.
 162 Median species richness and the range of species richness values per site is similar across vegetation
 163 types (Table 1).

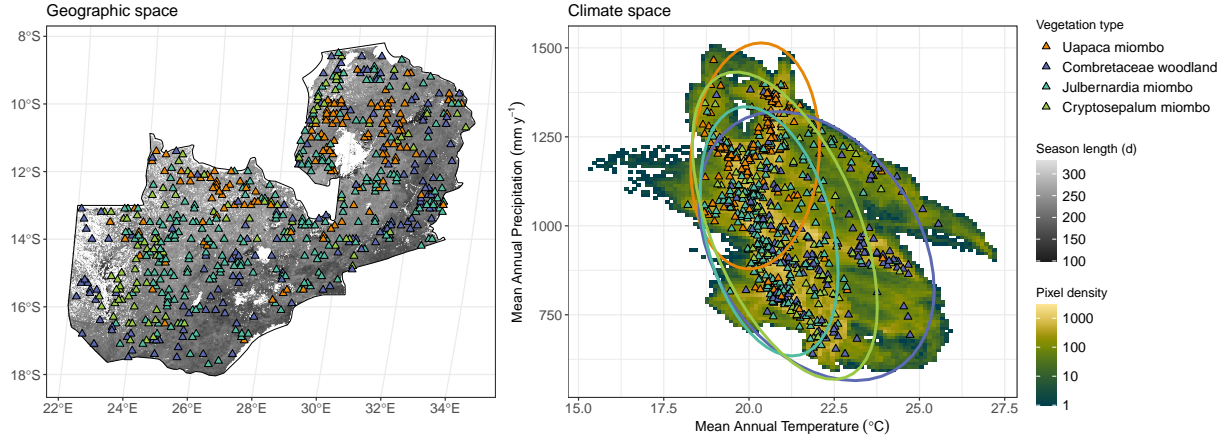


Figure 2: Distribution of study sites, within Zambia (left), and in climate space (right). Sites are shown as triangles, coloured according to vegetation type. Zambia is shaded according to mean growing season length during the period 2001 to 2021, estimated from the MODIS MCD12Q2 land surface phenology product, at 500 m spatial resolution (Friedl et al., 2022). Growing season length is masked by the MODIS MCD12Q1 land cover map from 2015 (Friedl & Sulla-Menashe, 2019), removing all pixels occurring in wetlands, croplands, water bodies, and urban areas. Climate space is represented by Mean Annual Temperature (MAT) and Mean Annual Precipitation (MAP), extracted from the WorldClim dataset at 30 arc second resolution (Fick & Hijmans, 2017). The shaded area in the right panel shows the climate space of Zambia, showing the density of pixels for given values of MAT and MAP. The ellipses in the right panel show the 95th percentiles of the climate space of each vegetation type.

Vegetation type	N sites	Richness	Indicator species	Indicator value
Uapaca miombo	135	17(7)	<i>Brachystegia longifolia</i>	0.393
			<i>Uapaca kirkiana</i>	0.384
			<i>Marquesia macroura</i>	0.278
Combretaceae woodland	144	14(5)	<i>Combretum molle</i>	0.258
			<i>Lannea discolor</i>	0.229
			<i>Combretum zeyheri</i>	0.212
Julbernardia miombo	244	17(6)	<i>Julbernardia paniculata</i>	0.556
			<i>Brachystegia boehmii</i>	0.540
			<i>Pseudolachnostylis maprouneifolia</i>	0.227
Cryptosepalum miombo	96	14(6)	<i>Brachystegia spiciformis</i>	0.582
			<i>Cryptosepalum exfoliatum</i>	0.285
			<i>Guibourtia coleosperma</i>	0.282

Table 1: Dufrêne-Legendre indicator species analysis for the vegetation type clusters, based on basal area weighted species abundances (Dufrêne & Legendre, 1997). The three species per cluster with the highest indicator values are shown alongside the median and interquartile range of site species richness and the number of sites within each cluster.

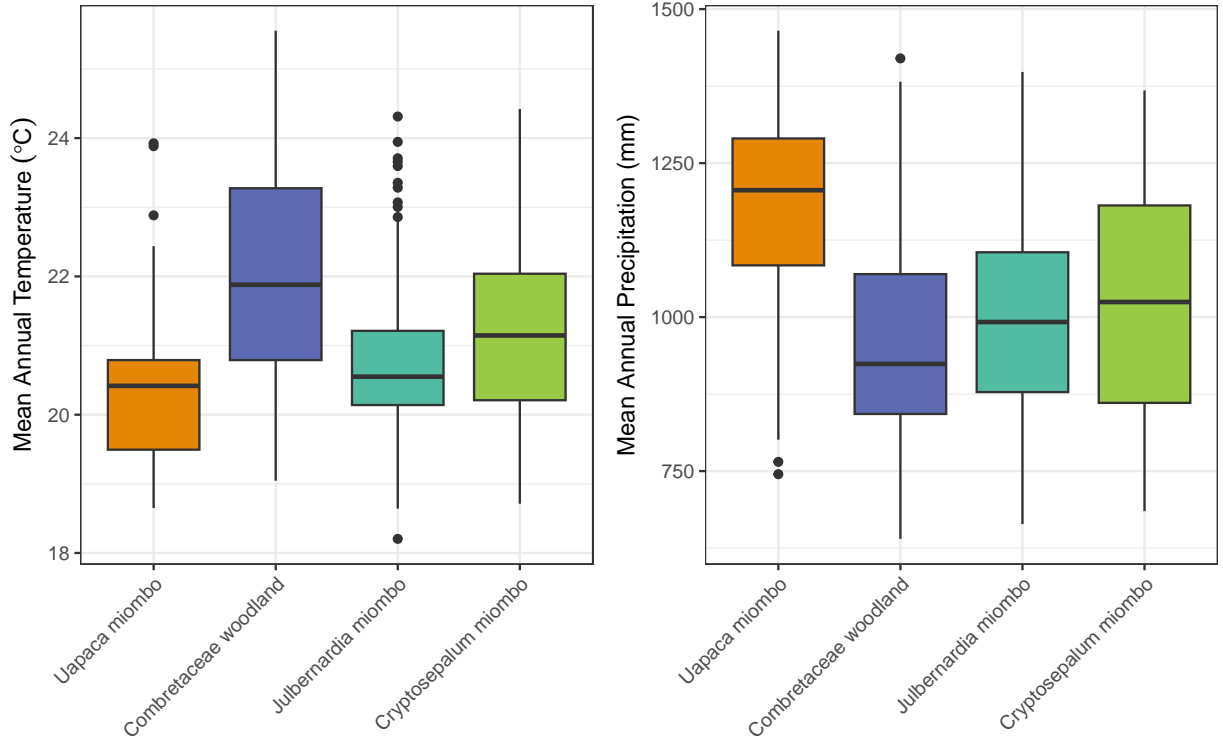


Figure 3: Mean Annual Precipitation and Mean Annual Temperature for each site, grouped by vegetation type. Climate data were extracted from the WorldClim dataset at 30 arc second resolution (Fick & Hijmans, 2017).

To describe species diversity in each site, we calculated the Shannon-Wiener index (H') from species basal area rather than individual abundance, as a measure of species diversity effectively weighted by species' contribution to canopy occupancy and thus the land surface phenological signal. H' was transformed to the first-order numbers-equivalent of H' (${}^1D = e^{H'}$), which gives the equivalent number of equally common species that would result in a given value of H' , also known as effective species richness (Jost, 2007). We use 1D as the primary measure of species diversity in our statistical models, and is subsequently referred to as species diversity. To describe the abundance of Detarioideae species we calculated their proportional basal area. To describe average tree size, we calculated the quadratic mean of stem diameters per site. Quadratic mean diameter is exactly related to site basal area, unlike the arithmetic mean of diameter, and assigns greater weight to larger trees (Curtis & Marshall, 2000). It is thus a more appropriate descriptor of average stem size for this study, where the arithmetic mean would be biased by an abundance of small stems, despite their small contribution to overall canopy land surface phenological signal.

2.3 Remote sensing data

Precipitation time series data for each site was compiled from the GPM IMERG Final Precipitation L3 1 day V06 product, which has a pixel size of 0.1° (11.1 km at the equator) (Huffman et al., 2015). We used all available data from 2001 to 2021. There is no clear consensus on best practice for defining the limits of the rainy season (Guan et al., 2014). Here we followed the example of Stern et al. (1981) and Adole et al. (2018b), variations of which have been used in other studies of African savanna-woodland phenology (Mupangwa et al., 2011; Segele & Lamb, 2005). First, we determined the temporal bounds of each wet-dry season cycle within our study period of 2001 to 2021 for each site according to Ferijal et al. (2022), as the 14 day period with the lowest precipitation in each calendar year. Where multiple 14 day periods tied for lowest precipitation within a single calendar year, the later period was chosen.

The onset of the rainy season for each wet-dry season cycle was defined as the start of the first period of 10 days with more than 20 mm total rainfall, immediately followed by 20 days with more than 30 mm total rainfall (Tadross et al., 2005). With this rolling window approach we sought to identify the first sustained period where plant available soil moisture was increasing, i.e. where the average regional evaporation rate of ~ 1 mm per day was exceeded by rainfall (Campbell, 1996), while accounting for the stochastic nature of rainfall in our study at the start of the rainy season. We chose to relax the rainfall constraint from 2 mm d^{-1} in the first 10 day period, to 1.5 mm d^{-1} for the subsequent 20 day period, to account for variation in the temporal consistency of rainfall at the start of the rainy season in our study region. As opposed to a percentile of cumulative rainfall approach, our method is not affected by dry season storm-burst rainfall events, which, while contributing to overall cumulative rainfall, often do not generally have the capacity to initiate tree foliage production due to their transience (February & Higgins, 2016).

The end of the rainy season was defined as the start of the first period where fewer than four days within a 30 day period received more than 0.5 mm rainfall. Guan et al. (2014) compares other methods of estimating rainy season onset and end dates, and finds little functional difference between the method chosen here and other common methods. To validate our delimitation of the rainy season we checked that all season start and end dates occurred within 10 days of the dates where 10% and 95% of yearly cumulative rainfall were surpassed, respectively (Adole et al., 2018b).

To quantify seasonal patterns of leaf display at each site, we used the MODIS MCD12Q2 v6.1 land surface phenology product (Friedl et al., 2022). MCD12Q2 provides annual metrics describing land surface phenology, with a spatial resolution of ~ 500 m. The phenological metrics in MCD12Q2 are derived from the 2-band Enhanced Vegetation Index time series (1-2 day temporal resolution), with nadir Bidirectional Reflectance Distribution Function-adjusted surface reflectance (NBAR-EVI2).

211 There are a number of land surface phenology products derived from MODIS vegetation indices.
212 MCD12Q2 was chosen here as it has been used effectively in other studies in deciduous African
213 woodlands to define the growing season (Begue et al., 2014; Adole et al., 2018a). Additionally, a
214 previous comparison of MODIS-derived land surface phenology products showed that MCD12Q2
215 out-performed other products in predicting the start of the growing season in relation to ground
216 observations (Peng et al., 2017).

217 All sites were determined to have a single annual growing season according to the MCD12Q2
218 “NumCycles” metric. We used all years of data from 2001 to 2021. We used the “Greenup”
219 and “Dormancy” metrics to define the growing season as the period when the EVI time series
220 exceeds 15% of the EVI amplitude for a given growing season (Figure 4). We used the “Maturity”
221 and “Senescence” metrics, defined as the dates bounding the period where the EVI time series
222 exceeds 90% of the EVI amplitude, to define the end of the green-up period and the start of the
223 senescence period, respectively. We used these dates to calculate the length of the green-up period
224 and senescence period. We calculated “pre-rain green-up” as the number of days between the onset
225 of the growing season and the onset of the rainy season, for each year of available data. Similarly we
226 calculated “senescence lag” as the number of days between the end of the rainy season and the end
227 of the growing season. To aid interpretation of statistical models, we reversed the sign of the pre-
228 rain green-up measurements, so that larger values indicate earlier pre-rain green-up. As senescence
229 generally occurred after the end of the rainy season, we did not reverse the sign of senescence lag,
230 so larger values indicate later senescence.

231 Daily total precipitation from the GPM IMERG product was separated into three periods of relev-
232 ance to different phenological metrics: precipitation during the growing season, precipitation in the
233 30 day period before the onset of the growing season (pre-green-up precipitation), and precipitation
234 in the 30 day period before the onset of senescence at the end of the growing season (pre-senescence
235 precipitation) (Figure 4).

236 Temperature time series data for each site was compiled from the ERA5-Land hourly data, using
237 the 2 m air temperature variable at 0.1°(11.1 km at the equator) (Muñoz-Sabater et al., 2021).
238 We aggregated these data to the maximum temperature for each day over the period 2001 to
239 2021. We then calculated cumulative temperature (degree days) during the 30 day pre-green-up
240 period, 30 day pre-senescence period, and the growing season period, as with the precipitation
241 data. Cumulative temperature has been shown in previous studies to be an important cue driving
242 patterns of leaf display in more temperate systems (Archibald & Scholes, 2007; Michelson et al.,
243 2017; Gárate-Escamilla et al., 2020). While the spatial scales of the climate data (0.1°) and land
244 surface phenology data (500 m) do not match we believe this does not present a problem for our
245 analyses. Firstly, because temperature and rainfall data are expressed in our analyses as cumulative

values across longer time periods, for example cumulative rainfall over the 30 days prior to green-up, we do not expect systematic spatial variation in these aggregated values within each 0.1° pixel, especially when considering multiple years of data. Secondly, the distance among sites is much greater than the resolution of the climate data. Any variation in temperature or rainfall within pixels is likely to be less than that among sites.

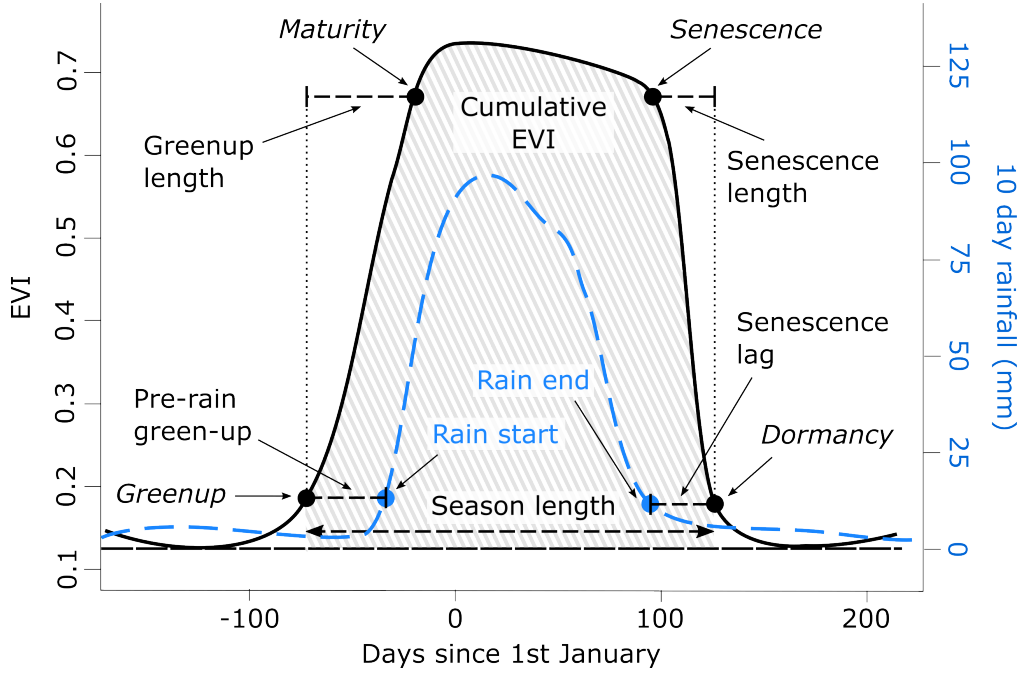


Figure 4: Schematic diagram of hypothetical splined NBAR-EVI2 time series (black curve), from which metrics provided by the MCD12Q2 product are derived (black circles), Adapted from Gray et al. (2022). Cumulative EVI is denoted by the shaded area under the EVI curve for a given growing season, bounded by the “Greenup” and “Dormancy” dates. The blue curve shows a hypothetical splined 10 day rolling total rainfall time series, derived from the GPM IMERG product. Blue circles indicate the start and end of the rainy season as defined by our algorithm. Dashed black lines indicate the derived phenological metrics used in this study. In this hypothetical example, “Greenup” occurs in advance of the start of the rainy season, and “Dormancy” occurs after the end of the rainy season, reflecting the condition of 72.7% (8451/11 625) of the yearly data in our dataset. In 26.7% (3106/11 625) of cases, dormancy occurred after the end of the rainy season and green-up occurred after the start of the rainy season. In 0.6% (68/11 625) of cases, dormancy occurred before the end of the rainy season.

2.3.1 Statistical modelling

Linear mixed effects models were used to investigate the effect of tree species diversity (effective number of species), species composition (relative abundance of detarioid species), and woodland structure (quadratic mean of stem diameter) on each of the six phenological metrics (cumulative

EVI, season length, length of green-up period, length of senescence period, pre-rain green-up, senescence lag). We specified a maximal model structure including the fixed effects of species diversity, quadratic mean of stem diameter, relative abundance of detarioid species, precipitation and cumulative temperature, the latter two of which have been shown by previous studies to strongly influence patterns of foliage display, including green-up and senescence (Whitecross et al., 2017; Adole et al., 2019). For models of growing season length and cumulative EVI we used cumulative rainy season precipitation and temperature; for pre-rain green-up and length of green-up period we used cumulative pre-green-up precipitation and temperature; for senescence lag and length of senescence period we used cumulative pre-senescence precipitation and temperature. All models included a random intercept term for site to account for yearly repeated measurements of site land surface phenology. Fixed effects in each model were standardised to Z-scores prior to modelling to allow comparison of slope coefficients within models.

To determine the magnitude and direction of each fixed effect on each phenological metric, we compared standardised effect sizes extracted from models re-estimated using Maximum Likelihood. For each fixed effect we calculated the 95% confidence interval of the effect size as $1.96 \times$ the standard error of the parameter estimate (Zuur et al., 2010). All statistical analyses were conducted in R version 4.0.2 (R Core Team, 2020).

3 Results

The majority of sites experienced pre-rain green-up, with the site mean date of green-up occurring in advance of the mean onset of the rainy season in 498/619 sites. Across all sites, the mean lag between green-up and the onset of seasonal rains was 14 ± 20.2 days (± 1 standard deviation). Linear mixed effects models effectively explained pre-rain green-up ($R^2_m=0.45$, $R^2_c=0.65$), cumulative EVI ($R^2_m=0.21$, $R^2_c=0.72$), green-up length ($R^2_m=0.20$, $R^2_c=0.38$) and season length ($R^2_m=0.14$, $R^2_c=0.63$), while senescence length ($R^2_m=0.01$, $R^2_c=0.20$) and senescence lag ($R^2_m=0.03$, $R^2_c=0.30$), were poorly explained. Fixed effects accounted the majority of total variance explained in models for pre-rain green-up, season length and green-up length, while the random effect of site explained most of the variance in cumulative EVI (Table S1).

We compared standardised fixed effect sizes for each phenological metric to determine the strength and direction of their influence (Figure 5). Tree species diversity exhibited positive effects on season length ($\beta=4.7 \pm 0.70$, standardised coefficient \pm standard error) (H_1) and pre-rain green-up ($\beta=1.0 \pm 0.39$) (H_2). Average tree size, measured by the quadratic mean of stem diameter per site, was a significant predictor of pre-rain green-up ($\beta=2.0 \pm 0.38$) and green-up length ($\beta=1.0 \pm 0.33$), associated with early pre-rain green-up and a longer green-up period (H_3). Sites with larger trees

also experienced later senescence ($\beta=0.8\pm0.67$). The proportional basal area of detarioid species was a significant predictor of pre-rain green-up ($\beta=1.0\pm0.40$), and season length ($\beta=1.7\pm0.71$) (H_4).

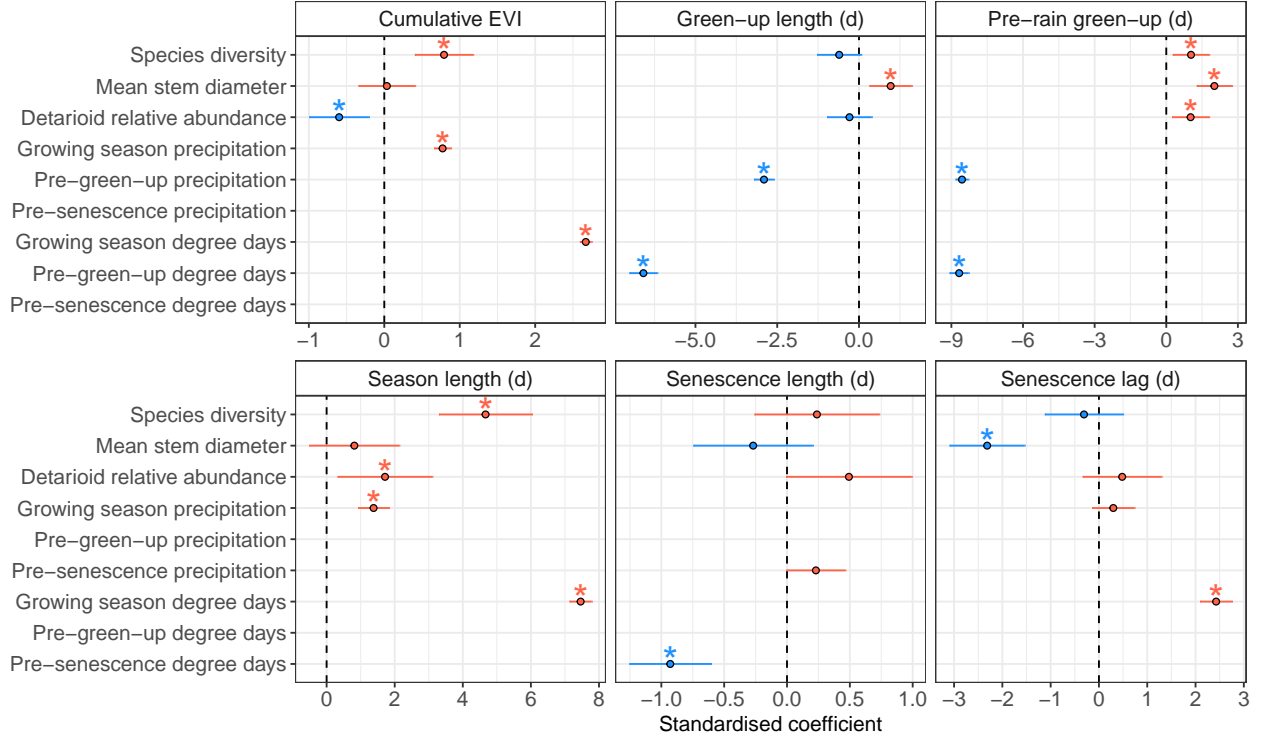


Figure 5: Standardised fixed effect coefficients (dots) with 95% confidence intervals (whiskers) for models of each phenological metric (panels). Estimates where the 95% confidence interval does not overlap zero are considered to be significant and are marked by asterisks. Temperature (degree days) and precipitation data were summed over different periods most relevant to each phenological metric. Green-up length and pre-rain green-up used data from the 30 day pre-green-up period, senescence length and senescence lag used data from the 30 day pre-senescence period, cumulative EVI and season length used data from the growing season period.

4 Discussion

We have demonstrated clear effects of tree species diversity, composition and structure on various metrics of land surface phenology in seasonally dry tropical woodlands across Zambia. Both tree species diversity and the proportional basal area of trees from the Detarioideae (subfamily of Fabaceae), were associated with a longer growing season and with earlier pre-rain green-up. Our models partition the effects of species diversity and detarioid relative abundance, suggesting that while some of the positive species diversity effect is due to niche complementarity, i.e. a true diversity effect, some is due to the increased likelihood of containing species able to green-up earlier, i.e. a mass-ratio effect (Grime, 1998; Tilman et al., 2014). Our study lends support for a gen-

299 eral positive effect of tree species diversity on ecosystem function in southern African seasonally dry
300 tropical woodlands, measured through leaf display (Richardson et al., 2009), which aligns with other
301 recent studies in the region (Godlee et al., 2021; McNicol et al., 2018; Shirima et al., 2015). Our
302 results highlight the important role of detarioid species in southern African woodland productivity:
303 we show that increasing abundance of these species increases both early season productivity and
304 overall growing season length.

305 The basal area of detarioid species had a positive effect on pre-rain green-up. Our results suggest a
306 mass-ratio effect in the pre-rain green-up of Zambian deciduous woodlands (Grime, 1998), whereby
307 a dominant functional group of trees with particular traits and life history strategy is able to green-
308 up in advance of seasonal rains and drive longer growing seasons. Given their tendency to create
309 deep root networks which provide effective water and non-structural carbohydrate storage (Zhou
310 et al., 2020; Timberlake & Calvert, 1993), and their high wood density which confers embolism-
311 resistance to the tree hydraulic system (Hoffmann et al., 2011; Hacke et al., 2001; Chave et al.,
312 2009), we suggest that compared to other co-occurring taxonomic groups, detarioid species are
313 better equipped to green-up before seasonal rainfall begins (Vinya et al., 2018). In our analysis we
314 accounted for the effect of tree size on pre-rain green-up, which generally correlates with rooting
315 depth, and still found an effect of detarioid abundance on pre-rain green-up, implying a true effect of
316 detarioid species not linked to tree size. While pre-rain green-up is a risky strategy, it may provide
317 a competitive advantage for detarioid species, allowing them to take advantage of early rainfall and
318 associated soil nutrient release (February & Higgins, 2016).

319 While at present the ability to green-up prior to the rainy season provides a competitive advantage
320 to detarioid species by extending the period of productivity, it is unclear whether this behaviour
321 will continue to provide a benefit under a changing climate, where the timing of the rainy season is
322 expected to shift, becoming more erratic and shorter overall (Shongwe et al., 2011; Pohl et al., 2017;
323 Wainwright et al., 2021). Given the dominance of detarioid species in miombo woodlands across
324 southern Africa, decreased productivity of this group due to a mismatch between leaf display and
325 seasonal rainfall may affect the future composition, structure and functioning of these woodlands,
326 potentially leading to a shorter stature, lower biomass and lower productivity ecosystem.

327 Environmental variables had consistently strong effects on phenological metrics, and confirm pre-
328 vious research. Greater rainfall within the rainy season led to a longer growing season and greater
329 cumulative EVI, matching our expectations that increased water availability allows for greater fo-
330 liage production and builds groundwater reserves allowing for a longer growing season (Adole et al.,
331 2018b). Surprisingly, greater rainfall in the 30 days leading up to the start of the growing season
332 was associated with later green-up with respect to the onset of the rainy season. We suggest this
333 may be the result of large amounts of rainfall kick-starting foliage production in the absence of

334 a pre-rain green-up effect in some sites, and may represent cases where grasses drive the start of
 335 growing season land surface phenology signal. This inability to discriminate between the grassy
 336 component and the tree canopy component of the phenological signal highlights one of the prin-
 337 ciple drawbacks with space-borne land surface phenology to characterise patterns of vegetation leaf
 338 display (Archibald & Scholes, 2007). Hotter days were associated with shorter periods of senes-
 339 cence and green-up, but ultimately a longer growing season and greater overall productivity. In
 340 the case of green-up length, this effect may imply a temperature trigger on leaf display, as is seen
 341 in temperate woodland ecosystems (Flynn & Wolkovich, 2018). In the case of senescence, hotter
 342 days at the end of the growing season are expected to increase photorespiration and ultimately
 343 result in a negative leaf carbon balance, triggering leaf loss (Warren et al., 2011; Mariën et al.,
 344 2019). This study provides a glimpse into how climate change, particularly warming (Arias et al.,
 345 2021) and increased rainfall seasonality (Wainwright et al., 2021), could affect leaf phenology in the
 346 future in southern Africa. Future temperature increases in miombo woodlands, particularly high
 347 temperatures at the start and end of the rainy season, could accelerate green-up and senescence
 348 processes. Similarly, a reduction in precipitation during the growing season could reduce growing
 349 season length and overall productivity. Future studies could explore further how climate extremes
 350 affect land surface phenology, ideally in combination with measurements of species composition and
 351 ecosystem structure, which this study has shown are also important drivers of ecosystem function.
 352 The end of the growing season came later with respect to the end of the rainy season in plots with
 353 larger mean stem diameter, though our model had low explanatory power. Cho et al. (2017) found
 354 that tree cover, measured by MODIS Leaf Area Index (LAI) data, had a significant positive effect
 355 on end of growing season date in tropical dry woodlands in South Africa. Similarly, Guan et al.
 356 (2014) found at continental scale across Africa that the end of the growing season came later with
 357 respect to the end of the rainy season in areas where tree cover was higher. Both these previous
 358 studies posit that the observed effect of tree cover on end of growing season date might indicate
 359 the presence of larger trees capable of accessing deeper groundwater reserves or holding stem-water
 360 reserves after the rainy season ends and surface soil moisture is depleted. Our study lends further
 361 support for this suggestion by directly testing the effect of tree size, rather than tree cover.
 362 Our best models predicting the length of the senescence period and the end of growing season
 363 lag did not explain much of the variance in these phenological metrics. Short term oscillations
 364 in soil moisture driven by localised rainfall events, and the condition of ground cover vegetation
 365 may be responsible for driving the length of the senescence period, hence the wide spatio-temporal
 366 variability of this phenological metric and the poor fit of our statistical models. Most of the variance
 367 explained by our models of senescence period length and senescence lag came from the random effect
 368 of site, implying some unmeasured inter-site variation. Grass productivity is more reactive to short-

term changes in soil moisture than tree activity, and may oscillate within the senescence period (Archibald & Scholes, 2007). This may explain the lack of a strong growing season precipitation or tree diversity signal for senescence lag and length of the senescence period in our models.

Other studies, both globally and within southern African woodlands, have largely ignored patterns of senescence, instead focussing on patterns of green-up (Gallinat et al., 2015). Most commonly, studies of senescence simply correlate the decline of rainfall with senescence (Stevens et al., 2016; Guan et al., 2014), but our best model suggests that temperature is a stronger determinant of the end of the growing season than precipitation. We suggest that hotter days at the end of the growing season might accelerate senescence through tissue damage and embolism (Cho et al., 2017), resulting in a shorter period of senescence. In temperate ecosystems, which experience autumn senescence, lower night time temperatures have been shown to increase the rate of senescence and thus decrease senescence period length (Michelson et al., 2017; Gárate-Escamilla et al., 2020). In these water-limited and hot systems however, it seems hotter temperatures are the main driver of senescence. Hotter days prior to senescence appear to delay the onset of senescence with respect to the end of the rainy season, and higher temperatures across the growing season were associated with a longer growing season. Thus, while climate warming could accelerate the process of senescence, it may also delay the senescence period with respect to the end of the rainy season.

Alternatively, Zani et al. (2020) suggests that in resource-limited environments, senescence times may largely be set by preceding photosynthetic activity and sink-limitations on growth. For example, limited nutrient supply may prohibit photosynthesis late in the season if the preceding photosynthetic activity has depleted that supply. Reich et al. (1992) suggested that there are many direct constraints on leaf life-span such as drought and herbivory, especially in the seasonally dry tropics, which would lead to timing of senescence being set largely by the time of bud-burst. Our study indirectly corroborates this theory, with the finding of a moderate negative correlation between pre-rain green-up and senescence lag across all vegetation types indicating that later green-up allows later senescence (Figure S1).

We found positive effects of tree size (site quadratic mean diameter) on pre-rain green-up and green-up length, but negative effects on senescence lag. Our results agree with previous studies that the increased rooting depth of large trees allows them to access deep ground-water reserves, conferring resilience to inter-annual variation in patterns of seasonal rainfall (Holdo et al., 2017). While detarioid species in these woodlands tend to grow to large sizes, our result of a significant effect of tree size alongside an effect of detarioid abundance on pre-rain green-up infers particular traits beyond tree size in the detarioid species that drive pre-rain green-up.

Our finding that species diversity increases growing season length and cumulative EVI in seasonally dry tropical woodlands provides an example of a mechanism by which species diversity increases

ecosystem function, a pattern observed previously in other studies of southern African woodlands (Godlee et al., 2021; McNicol et al., 2018; Shirima et al., 2015), and globally in other biomes (van der Plas, 2019; Tilman et al., 2014). Our findings provide earth system modellers with an insight to better understand how changes in the inter-related variables of species diversity, composition and structure affect one measure of ecosystem function (land surface phenology). Future studies should aim to disentangle these effects further, possibly in an experimental context. Incorporating predictions of biotic composition and its change over time into earth system models has been limited until recently for two main reasons. Firstly, there are large uncertainties in the effects of biodiversity on ecosystem function, e.g. gross primary productivity (GPP) (Ahlstrom et al., 2015). Secondly, until recently there has been a major paucity of ground data on community composition, and a lack of appropriate remote-sensing data to scale up to larger areas (van Bodegom et al., 2011). Our study comes at a pertinent time where plot-based vegetation monitoring networks are now sufficiently widespread to robustly test hypotheses and generate theory on the effects of community composition on ecosystem function across environmental gradients (ForestPlots.net et al., 2021; SEOSAW, 2020). Additionally, recent advances in remote sensing of functional diversity from hyperspectral data, combined with the imminent deployment of space-borne imaging spectrometers by multiple space agencies (Cawse-Nicholson et al., 2021; Rast et al., 2021), will soon allow community composition to be mapped at large spatial scales (Wallis et al., 2024; Cavender-Bares et al., 2020) and utilised by earth system modellers. Our study serves as an example of the kinds of advancements in ecological understanding relevant to earth system modelling that can be made by integrating abundant ground data and remote sensing data.

5 Conclusion

We explored how tree species diversity, composition and structure of seasonally dry tropical woodlands influence land surface phenology across Zambia. We showed that species diversity drives longer growing seasons and promotes earlier pre-rain green-up across woodlands in the miombo ecoregion. The abundance of Detarioideae species (subfamily of Fabaceae) had a positive effect on pre-rain green-up and growing season length, supporting suggestions from previous studies of their important role in driving pre-rain green-up in southern African miombo woodlands. Finally, we found that larger trees drive earlier pre-rain green-up supporting previous research suggesting that deep roots and persistent carbohydrate storage allows for precocious leaf display.

Our results lend further support to an already well established corpus of study on the positive effect of species diversity on ecosystem function. Additionally, our results provide evidence for earth-system modellers, demonstrating the importance of structure and diversity in determining patterns

of land surface phenology. As reliable data on ecosystem structure, particularly tree size, become available across larger spatial scales and at higher spatial resolution, we hope that these data can be explored in models of land-atmosphere mass and energy exchange to improve their predictive skill under a changing climate.

References

- Adole, T., J. Dash & P. M. Atkinson (2018a). ‘Characterising the land surface phenology of Africa using 500 m MODIS EVI’. In: *Applied Geography* 90, pp. 187–199. DOI: 10.1016/j.apgeog.2017.12.006.
- Adole, T., J. Dash & P. M. Atkinson (2018b). ‘Large-scale prerain vegetation green-up across Africa’. In: *Global Change Biology* 24.9, pp. 4054–4068. DOI: 10.1111/gcb.14310.
- Adole, T., J. Dash, V. Rodriguez-Galiano & P. M. Atkinson (2019). ‘Photoperiod controls vegetation phenology across Africa’. In: *Communications Biology* 2.1. DOI: 10.1038/s42003-019-0636-7.
- Ahlstrom, A., M. R. Raupach, G. Schurgers, B. Smith, A. Arneth, M. Jung, M. Reichstein, J. G. Canadell, P. Friedlingstein, A. K. Jain et al. (2015). ‘The dominant role of semi-arid ecosystems in the trend and variability of the land CO₂ sink’. In: *Science* 348.6237, pp. 895–899. DOI: 10.1126/science.aaa1668.
- de Araujo, H. F. P., A. H. Vieira-Filho, M. R. V. Barbosa, J. A. F. Diniz-Filho & J. M. C. da Silva (2017). ‘Passerine phenology in the largest tropical dry forest of South America: Effects of climate and resource availability’. In: *Emu - Austral Ornithology* 117.1, pp. 78–91. DOI: 10.1080/01584197.2016.1265430.
- Archibald, S. & R. J. Scholes (2007). ‘Leaf green-up in a semi-arid African savanna -separating tree and grass responses to environmental cues’. In: *Journal of Vegetation Science* 18.4, pp. 583–594. DOI: 10.1111/j.1654-1103.2007.tb02572.x.
- Arias, P., N. Bellouin, E. Coppola, R. Jones, G. Krinner, J. Marotzke, V. Naik, M. Palmer, G.-K. Plattner, J. Rogelj et al. (2021). ‘Technical Summary’. In: *Climate Change 2021: The Physical Science Basis. Contribution of Working Group I to the Sixth Assessment Report of the Intergovernmental Panel on Climate Change*. Ed. by V. Masson-Delmotte, P. Zhai, A. Pirani, S. Connors, C. Péan, S. Berger, N. Caud, Y. Chen, L. Goldfarb, M. Gomis et al. Cambridge, United Kingdom and New York, NY, USA: Cambridge University Press, pp. 33–144. DOI: 10.1017/9781009157896.002.
- Bale, J. S., G. J. Masters, I. D. Hodkinson, C. Awmack, T. M. Bezemer, V. K. Brown, J. Butterfield, A. Buse, J. C. Coulson, J. Farrar et al. (2002). ‘Herbivory in global climate change research: direct effects of rising temperature on insect herbivores’. In: *Global Change Biology* 8.1, pp. 1–16. DOI: 10.1046/j.1365-2486.2002.00451.x.

471 Begue, A., E. Vintrou, A. Saad & P. Hiernaux (September 2014). ‘Differences between cropland
 472 and rangeland MODIS phenology (start-of-season) in Mali’. In: *International Journal of Applied*
 473 *Earth Observation and Geoinformation* 31, pp. 167–170. DOI: 10.1016/j.jag.2014.03.024.

474 Bloom, A. A., J. Exbrayat, I. R. van der Velde, L. Feng & M. Williams (2016). ‘The decadal
 475 state of the terrestrial carbon cycle: Global retrievals of terrestrial carbon allocation, pools, and
 476 residence times’. In: *Proceedings of the National Academy of Sciences* 113.5, pp. 1285–1290. DOI:
 477 10.1073/pnas.1515160113.

478 van Bodegom, P. M., J. C. Douma, J. P. M. Witte, J. C. Ordoñez, R. P. Bartholomeus & R. Aerts
 479 (2011). ‘Going beyond limitations of plant functional types when predicting global ecosystem-
 480 atmosphere fluxes: exploring the merits of traits-based approaches’. In: *Global Ecology and Biogeo-*
 481 *graphy* 21.6, pp. 625–636. DOI: 10.1111/j.1466-8238.2011.00717.x.

482 Broadhead, J. S., C. K. Ong & C. R. Black (2003). ‘Tree phenology and water availability in
 483 semi-arid agroforestry systems’. In: *Forest Ecology and Management* 180.1-3, pp. 61–73. DOI:
 484 10.1016/s0378-1127(02)00602-3.

485 Campbell, B. M., ed. (1996). *The miombo in transition: Woodlands and welfare in Africa*. Bogor,
 486 Indonesia: Centre for International Forestry Research.

487 Cavender-Bares, J., J. A. Gamon & P. A. Townsend, eds. (2020). *Remote Sensing of Plant Biod-*
 488 *iversity*. Springer International Publishing. DOI: 10.1007/978-3-030-33157-3.

489 Cawse-Nicholson, K., P. A. Townsend, D. Schimel, A. M. Assiri, P. L. Blake, M. F. Buongiorno, P.
 490 Campbell, N. Carmon, K. A. Casey, R. E. Correa-Pabón et al. (2021). ‘NASA’s surface biology
 491 and geology designated observable: A perspective on surface imaging algorithms’. In: *Remote*
 492 *Sensing of Environment* 257, p. 112349. DOI: 10.1016/j.rse.2021.112349.

493 Chave, J., D. Coomes, S. Jansen, S. L. Lewis, N. G. Swenson & A. E. Zanne (2009). ‘Towards a
 494 worldwide wood economics spectrum’. In: *Ecology Letters* 12, pp. 351–366. DOI: 10.1111/j.1461-
 495 0248.2009.01285.x.

496 Chidumayo, E. N. (2001). ‘Climate and phenology of savanna vegetation in southern Africa’. In:
 497 *Journal of Vegetation Science* 12.3, p. 347. DOI: 10.2307/3236848.

498 Cho, M. A., A. Ramoelo & L. Dziba (2017). ‘Response of land surface phenology to variation in
 499 tree cover during green-up and senescence periods in the semi-arid savanna of southern Africa’.
 500 In: *Remote Sensing* 9.7, p. 689. DOI: 10.3390/rs9070689.

501 Cole, E. F., P. R. Long, P. Zelazowski, M. Szulkin & B. C. Sheldon (2015). ‘Predicting bird phenology
 502 from space: Satellite-derived vegetation green-up signal uncovers spatial variation in phenological
 503 synchrony between birds and their environment’. In: *Ecology and Evolution* 5.21, pp. 5057–5074.
 504 DOI: 10.1002/ece3.1745.

505 Cook, B. I., J. S. Mankin, K. Marvel, A. P. Williams, J. E. Smerdon & K. J. Anchukaitis (2020).
506 ‘Twenty-First Century Drought Projections in the CMIP6 Forcing Scenarios’. In: *Earth’s Future*
507 8.6. DOI: 10.1029/2019ef001461.

508 Curtis, R. O. & D. D. Marshall (2000). ‘Technical Note: Why Quadratic Mean Diameter?’ In:
509 *Western Journal of Applied Forestry* 15.3, pp. 137–139. DOI: 10.1093/wjaf/15.3.137.

510 Dahlin, K. M., D. Del Ponte, E. Setlock & R. Nagelkirk (2016). ‘Global patterns of drought deciduous
511 phenology in semi-arid and savanna-type ecosystems’. In: *Ecography* 40.2, pp. 314–323. DOI: 10.
512 1111/ecog.02443.

513 Dinerstein, E., D. Olson, A. Joshi, C. Vynne, N. D. Burgess, E. Wikramanayake, N. Hahn, S.
514 Palminteri, P. Hedao, R. Noss et al. (2017). ‘An ecoregion-based approach to protecting half the
515 terrestrial realm’. In: *BioScience* 67.6, pp. 534–545. DOI: 10.1093/biosci/bix014.

516 Dufrêne, M. & P. Legendre (1997). ‘Species assemblage and indicator species: The need for a flex-
517 ible asymmetrical approach’. In: *Ecological Monographs* 67, pp. 345–366. DOI: 10.1890/0012-
518 9615(1997)067[0345:SAIST]2.0.CO;2.

519 Faith, D. P., P. R. Minchin & L. Belbin (1987). ‘Compositional dissimilarity as a robust measure of
520 ecological distance’. In: *Vegetatio* 69.1-3, pp. 57–68. DOI: 10.1007/bf00038687.

521 Fayolle, A., M. D. Swaine, J. Bastin, N. Bourland, J. A. Comiskey, G. Dauby, J. Doucet, J. Gillet,
522 S. Gourlet-Fleury, O. J. Hardy et al. (2014). ‘Patterns of tree species composition across tropical
523 African forests’. In: *Journal of Biogeography* 41.12, pp. 2320–2331. DOI: 10.1111/jbi.12382.

524 February, E. C. & S. I. Higgins (2016). ‘Rapid Leaf Deployment Strategies in a Deciduous Savanna’.
525 In: *PLoS ONE* 11.6. Ed. by B. Bond-Lamberty, e0157833. DOI: 10.1371/journal.pone.0157833.

526 Ferijal, T., O. Batelaan, M. Shanafield & F. Alfahmi (2022). ‘Determination of rainy season onset
527 and cessation based on a flexible driest period’. In: *Theoretical and Applied Climatology* 148.1-2,
528 pp. 91–104. DOI: 10.1007/s00704-021-03917-1.

529 Fick, S. E. & R. J. Hijmans (2017). ‘WorldClim 2: New 1-km spatial resolution climate surfaces for
530 global land areas’. In: *International Journal of Climatology* 37.12, pp. 4302–4315. DOI: 10.1002/
531 joc.5086.

532 Flynn, D. F. B. & E. M. Wolkovich (2018). ‘Temperature and photoperiod drive spring phenology
533 across all species in a temperate forest community’. In: *New Phytologist* 219.4, pp. 1353–1362.
534 DOI: 10.1111/nph.15232.

535 ForestPlots.net, C. Blundo, J. Carilla, R. Grau, A. Malizia, L. Malizia, O. Osinaga-Acosta, M.
536 Bird, M. Bradford, D. Catchpole et al. (2021). ‘Taking the pulse of Earth’s tropical forests using
537 networks of highly distributed plots’. In: *Biological Conservation* 260, p. 108849. DOI: 10.1016/
538 j.biocon.2020.108849.

539 Friedl, M. & D. Sulla-Menashe (2019). *MCD12Q1 MODIS/Terra+Aqua Land Cover Type Yearly L3*
540 *Global 500m SIN Grid V006 [Data set]*. NASA EOSDIS Land Processes DAAC. DOI: 10.5067/
541 MODIS/MCD12Q1.006. (Visited on 23/07/2021).

542 Friedl, M., J. Gray & D. Sulla-Menashe (2022). *MODIS/Terra+Aqua Land Cover Dynamics Yearly*
543 *L3 Global 500m SIN Grid V061*. DOI: 10.5067/MODIS/MCD12Q2.061. (Visited on 01/03/2023).

544 Fuller, D. O. (1999). ‘Canopy phenology of some mopane and miombo woodlands in eastern Zambia’.
545 In: *Global Ecology and Biogeography* 8.3-4, pp. 199–209. DOI: 10.1046/j.1365-2699.1999.
546 00130.x.

547 Gallinat, A. S., R. B. Primack & D. L. Wagner (2015). ‘Autumn, the neglected season in climate
548 change research’. In: *Trends in Ecology & Evolution* 30.3, pp. 169–176. DOI: 10.1016/j.tree.
549 2015.01.004.

550 Gárate-Escamilla, H., C. C. Brelsford, A. Hampe, T. M. Robson & M. B. Garzón (2020). ‘Greater
551 capacity to exploit warming temperatures in northern populations of European beech is partly
552 driven by delayed leaf senescence’. In: *Agricultural and Forest Meteorology* 284, p. 107908. DOI:
553 10.1016/j.agrformet.2020.107908.

554 Garonna, I., R. de Jong & M. E. Schaepman (2016). ‘Variability and evolution of global land surface
555 phenology over the past three decades (1982-2012)’. In: *Global Change Biology* 22.4, pp. 1456–
556 1468. DOI: 10.1111/gcb.13168.

557 Giraldo, J. P. & N. M. Holbrook (2011). ‘Physiological mechanisms underlying the seasonality of leaf
558 senescence and renewal in seasonally dry tropical forest trees’. In: *Seasonally Dry Tropical Forests*.
559 Island Press/Center for Resource Economics, pp. 129–140. DOI: 10.5822/978-1-61091-021-7_8.

560 Godlee, J. L., C. M. Ryan, D. Bauman, S. J. Bowers, J. M. B. Carreiras, A. V. Chisingui, J. P. G. M.
561 Crooms, D. J. Druce, M. Finckh, F. M. Gonçalves et al. (2021). ‘Structural diversity and tree
562 density drives variation in the biodiversity-ecosystem function relationship of woodlands and
563 savannas’. In: *New Phytologist* 232.2, pp. 579–594. DOI: 10.1111/nph.17639.

564 Gore, M., B. J. Abiodun & F. Kucharski (2019). ‘Understanding the influence of ENSO patterns on
565 drought over southern Africa using SPEEDY’. In: *Climate Dynamics* 54.1-2, pp. 307–327. DOI:
566 10.1007/s00382-019-05002-w.

567 Gray, J., D. Sulla-Menashe & M. A. Friedl (2022). *User Guide to Collection 6.1 MODIS Land Cover*
568 *Dynamics (MCD12Q2) Product*. Accessed: 1st March 2023. URL: [https://lpdaac.usgs.gov/
569 documents/1417/MCD12Q2_User_Guide_V61.pdf](https://lpdaac.usgs.gov/documents/1417/MCD12Q2_User_Guide_V61.pdf).

570 Grime, J. P. (1998). ‘Benefits of plant diversity to ecosystems: Immediate, filter and founder effects’.
571 In: *Journal of Ecology* 86.6, pp. 902–910. DOI: 10.1046/j.1365-2745.1998.00306.x.

572 Gu, L., W. M. Post, D. Baldocchi, T. A. Black, S. B. Verma, T. Vesala & S. C. Wofsy (2003).
573 ‘Phenology of vegetation photosynthesis’. In: *Phenology: An Integrative Environmental Science*,
574 pp. 467–485. DOI: 10.1007/978-94-007-0632-3_29.

575 Guan, K., E. F. Wood, D. Medvigy, J. Kimball, M. Pan, K. K. Caylor, J. Sheffield, C. Xu & M. O.
576 Jones (2014). ‘Terrestrial hydrological controls on land surface phenology of African savannas
577 and woodlands’. In: *Journal of Geophysical Research: Biogeosciences* 119.8, pp. 1652–1669. DOI:
578 10.1002/2013jg002572.

579 Hacke, U. G., J. S. Sperry, W. T. Pockman, S. D. Davis & K. A. McCulloh (2001). ‘Trends in
580 wood density and structure are linked to prevention of xylem implosion by negative pressure’. In:
581 *Oecologia* 126.4, pp. 457–461. DOI: 10.1007/s004420100628.

582 Helman, D. (2018). ‘Land surface phenology: What do we really ‘see’ from space?’ In: *Science of*
583 *The Total Environment* 618, pp. 665–673. DOI: 10.1016/j.scitotenv.2017.07.237.

584 Hoffmann, W. A., R. M. Marchin, P. Abit & O. L. Lau (2011). ‘Hydraulic failure and tree dieback are
585 associated with high wood density in a temperate forest under extreme drought: Tree responses
586 to severe drought’. In: *Global Change Biology* 17.8, pp. 2731–2742. DOI: 10.1111/j.1365-
587 2486.2011.02401.x.

588 Holdo, R. M., J. B. Nippert & M. C. Mack (2017). ‘Rooting depth varies differentially in trees
589 and grasses as a function of mean annual rainfall in an African savanna’. In: *Oecologia* 186.1,
590 pp. 269–280. DOI: 10.1007/s00442-017-4011-4.

591 Huffman, G. J., E. F. Stocker, D. Bolvin, E. J. Nelkin & J. Tan (2015). *GPM IMERG Final*
592 *Precipitation L3 1 day 0.1 degree x 0.1 degree V06 [Data set]*. Goddard Earth Sciences Data
593 and Information Services Center (GES DISC). DOI: 10.5067/MODIS/MOD13Q1.006. (Visited on
594 30/10/2020).

595 Jeganathan, C., J. Dash & P. M. Atkinson (2014). ‘Remotely sensed trends in the phenology of
596 northern high latitude terrestrial vegetation, controlling for land cover change and vegetation
597 type’. In: *Remote Sensing of Environment* 143, pp. 154–170. DOI: 10.1016/j.rse.2013.11.020.

598 Jost, L. (2007). ‘Partitioning diversity into independent alpha and beta components’. In: *Ecology*
599 88.10, pp. 2427–2439. DOI: 10.1890/06-1736.1.

600 Keith, D. A., J. R. Ferrer-Paris, E. Nicholson & R. T. Kingsford, eds. (2020). *IUCN Global Ecosystem*
601 *Typology 2.0: Descriptive profiles for biomes and ecosystem functional groups*. IUCN, International
602 Union for Conservation of Nature. DOI: 10.2305/iucn.ch.2020.13.en.

603 Kreft, H. & W. Jetz (2010). ‘A framework for delineating biogeographical regions based on species
604 distributions’. In: *Journal of Biogeography* 37.11, pp. 2029–2053. DOI: 10.1111/j.1365-2699.
605 2010.02375.x.

606 Kushwaha, C., S. Tripathi, B. Tripathi & K. Singh (2011). ‘Patterns of tree phenological diversity in
607 dry tropics’. In: *Acta Ecologica Sinica* 31.4, pp. 179–185. DOI: 10.1016/j.chnaes.2011.04.003.

608 Lasky, J. R., M. Uriarte & R. Muscarella (2016). ‘Synchrony, compensatory dynamics, and the
609 functional trait basis of phenological diversity in a tropical dry forest tree community: effects of

rainfall seasonality'. In: *Environmental Research Letters* 11.11, p. 115003. DOI: 10.1088/1748-9326/11/11/115003.

Ma, X., X. Zhu, Q. Xie, J. Jin, Y. Zhou, Y. Luo, Y. Liu, J. Tian & Y. Zhao (2022). 'Monitoring nature's calendar from space: Emerging topics in land surface phenology and associated opportunities for science applications'. In: *Global Change Biology* 28.24, pp. 7186–7204. DOI: 10.1111/gcb.16436.

Makhado, R. A., M. J. Potgieter & W. J. Luus-Powell (2018). 'Colophospermum mopane leaf production and phenology in southern Africa's savanna ecosystem - a review'. In: *Insights of Forest Research* 2.1. DOI: 10.36959/948/464.

Mariën, B., M. Balzarolo, I. Dox, S. Leys, M. J. Lorène, C. Geron, M. Portillo-Estrada, H. AbdElgawad, H. Asard & M. Campioli (2019). 'Detecting the onset of autumn leaf senescence in deciduous forest trees of the temperate zone'. In: *New Phytologist* 224.1, pp. 166–176. DOI: 10.1111/nph.15991.

McNicol, I. M., C. M. Ryan, K. G. Dexter, S. M. J. Ball & M. Williams (2018). 'Aboveground carbon storage and its links to stand structure, tree diversity and floristic composition in south-eastern Tanzania'. In: *Ecosystems* 21, pp. 740–754. DOI: 10.1007/s10021-017-0180-6.

Michelson, I. H., P. K. Ingvarsson, K. M. Robinson, E. Edlund, M. E. Eriksson, O. Nilsson & S. Jansson (2017). 'Autumn senescence in aspen is not triggered by day length'. In: *Physiologia Plantarum* 162.1, pp. 123–134. DOI: 10.1111/pp1.12593.

Morellato, L. P. C., B. Alberton, S. T. Alvarado, B. Borges, E. Buisson, M. G. G. Camargo, L. F. Cancian, D. W. Carstensen, D. F. E. Escobar, P. T. P. Leite et al. (2016). 'Linking plant phenology to conservation biology'. In: *Biological Conservation* 195, pp. 60–72. DOI: 10.1016/j.biocon.2015.12.033.

Morellato, L. P. C., M. G. G. Camargo & E. Gressler (2013). 'A Review of Plant Phenology in South and Central America'. In: *Phenology: An Integrative Environmental Science*, pp. 91–113. DOI: 10.1007/978-94-007-6925-06.

Mukosha, J. & A. Siampale (2009). *Integrated land use assessment Zambia 2005–2008*. Lusaka, Zambia: Ministry of Tourism, Environment et al.

Muñoz-Sabater, J., E. Dutra, A. Agustí-Panareda, C. Albergel, G. Arduini, G. Balsamo, S. Boussetta, M. Choulga, S. Harrigan, H. Hersbach et al. (2021). 'ERA5-Land: a state-of-the-art global reanalysis dataset for land applications'. In: *Earth System Science Data* 13.9, pp. 4349–4383. DOI: 10.5194/essd-13-4349-2021.

Mupangwa, W., S. Walker & S. Twomlow (2011). 'Start, end and dry spells of the growing season in semi-arid southern Zimbabwe'. In: *Journal of Arid Environments* 75.11, pp. 1097–1104. DOI: 10.1016/j.jaridenv.2011.05.011.

645 Murtagh, F. & P. Legendre (2014). ‘Ward’s hierarchical agglomerative clustering method: Which
646 algorithms implement Ward’s criterion?’ In: *Journal of Classification* 31.3, pp. 274–295. DOI:
647 10.1007/s00357-014-9161-z.

648 Ogutu, J. O., H. Piepho & H. T. Dublin (2013). ‘Responses of phenology, synchrony and fecundity
649 of breeding by African ungulates to interannual variation in rainfall’. In: *Wildlife Research* 40.8,
650 p. 698. DOI: 10.1071/wr13117.

651 Pau, S., E. M. Wolkovich, B. I. Cook, T. J. Davies, N. J. B. Kraft, K. Bolmgren, J. L. Betancourt &
652 E. E. Cleland (2011). ‘Predicting phenology by integrating ecology, evolution and climate science’.
653 In: *Global Change Biology* 17.12, pp. 3633–3643. DOI: 10.1111/j.1365-2486.2011.02515.x.

654 Pavlick, R., D. T. Drewry, K. Bohn, B. Reu & A. Kleidon (2013). ‘The Jena Diversity-Dynamic
655 Global Vegetation Model (JeDi-DGVM): A diverse approach to representing terrestrial biogeo-
656 graphy and biogeochemistry based on plant functional trade-offs’. In: *Biogeosciences* 10.6, pp. 4137–
657 4177. DOI: 10.5194/bg-10-4137-2013.

658 Pelletier, J., A. Paquette, K. Mbindo, N. Zimba, A. Siampale, B. Chendauka, F. Siangulube &
659 J. W. Roberts (2018). ‘Carbon sink despite large deforestation in African tropical dry forests
660 (miombo woodlands)’. In: *Environmental Research Letters* 13, p. 094017. DOI: 10.1088/1748-
661 9326/aadc9a.

662 Peng, D., X. Zhang, C. Wu, W. Huang, A. Gonsamo, A. R. Huete, K. Didan, B. Tan, X. Liu &
663 B. Zhang (2017). ‘Intercomparison and evaluation of spring phenology products using National
664 Phenology Network and AmeriFlux observations in the contiguous United States’. In: *Agricultural
665 and Forest Meteorology* 242, pp. 33–46. DOI: 10.1016/j.agrformet.2017.04.009.

666 Penuelas, J., T. Rutishauser & I. Filella (2009). ‘Phenology feedbacks on climate change’. In: *Science*
667 324.5929, pp. 887–888. DOI: 10.1126/science.1173004.

668 van der Plas, F. (2019). ‘Biodiversity and ecosystem functioning in naturally assembled communit-
669 ies’. In: *Biological Reviews* 94, pp. 1220–1245. DOI: 10.1111/brv.12499.

670 Pohl, B., C. Macron & P.-A. Monerie (2017). ‘Fewer rainy days and more extreme rainfall by the
671 end of the century in southern Africa’. In: *Scientific Reports* 7.1. DOI: 10.1038/srep46466.

672 Prather, C. M., S. L. Pelini, A. Laws, E. Rivest, M. Woltz, C. P. Bloch, I. Del Toro, C. Ho,
673 J. Kominoski, T. A. S. Newbold et al. (2012). ‘Invertebrates, ecosystem services and climate
674 change’. In: *Biological Reviews* 88.2, pp. 327–348. DOI: 10.1111/brv.12002.

675 R Core Team (2020). *R: A Language and Environment for Statistical Computing*. R Foundation for
676 Statistical Computing. Vienna, Austria. URL: <https://www.R-project.org/>.

677 Rast, M., J. Nieke, J. Adams, C. Isola & F. Gascon (2021). ‘Copernicus Hyperspectral Imaging
678 Mission for the Environment (Chime)’. In: *2021 IEEE International Geoscience and Remote
679 Sensing Symposium IGARSS*, pp. 108–111. DOI: 10.1109/IGARSS47720.2021.9553319.

Reich, P. B., M. B. Walters & D. S. Ellsworth (1992). ‘Leaf life-span in relation to leaf, plant, and stand characteristics among diverse ecosystems’. In: *Ecological Monographs* 62.3, pp. 365–392. DOI: 10.2307/2937116.

Richardson, A. D., D. Y. Hollinger, D. B. Dail, J. T. Lee, J. W. Munger & J. O’Keefe (2009). ‘Influence of spring phenology on seasonal and annual carbon balance in two contrasting New England forests’. In: *Tree Physiology* 29.3, pp. 321–331. DOI: 10.1093/treephys/tpn040.

Richardson, A. D., T. F. Keenan, M. Migliavacca, Y. Ryu, O. Sonnentag & M. Toomey (2013). ‘Climate change, phenology, and phenological control of vegetation feedbacks to the climate system’. In: *Agricultural and Forest Meteorology* 169, pp. 156–173. DOI: 10.1016/j.agrformet.2012.09.012.

Rousseeuw, P. J. (1987). ‘Silhouettes: A graphical aid to the interpretation and validation of cluster analysis’. In: *Journal of Computational and Applied Mathematics* 20, pp. 53–65. DOI: 10.1016/0377-0427(87)90125-7.

Ryan, C. M., M. Williams, J. Grace, E. Woollen & C. E. R. Lehmann (2017). ‘Pre-rain green-up is ubiquitous across southern tropical Africa: implications for temporal niche separation and model representation’. In: *New Phytologist* 213.2, pp. 625–633. DOI: 10.1111/nph.14262.

Scheiter, S., L. Langan & S. I. Higgins (2013). ‘Next-generation dynamic global vegetation models: Learning from community ecology’. In: *New Phytologist* 198.3, pp. 957–969. DOI: 10.1111/nph.12210.

Segele, Z. T. & P. J. Lamb (2005). ‘Characterization and variability of Kiremt rainy season over Ethiopia’. In: *Meteorology and Atmospheric Physics* 89.1-4, pp. 153–180. DOI: 10.1007/s00703-005-0127-x.

SEOSAW (2020). ‘A network to understand the changing socio-ecology of the southern African woodlands (SEOSAW): Challenges, benefits, and methods’. In: *Plants, People, Planet* 3.3, pp. 249–267. DOI: 10.1002/ppp3.10168.

Seyednasrollah, B., A. M. Young, K. Hufkens, T. Milliman, M. A. Friedl, S. Froking & A. D. Richardson (2019). ‘Tracking vegetation phenology across diverse biomes using Version 2.0 of the PhenoCam Dataset’. In: *Scientific Data* 6.1. DOI: 10.1038/s41597-019-0229-9.

Shirima, D. D., M. Pfeifer, P. J. Platts, Ø. Totland & S. R. Moe (2015). ‘Interactions between canopy structure and herbaceous biomass along environmental gradients in moist forest and dry miombo woodland of Tanzania’. In: *PLoS ONE* 10, pp. 1–15. DOI: 10.1371/journal.pone.0142784.

Shongwe, M. E., G. J. van Oldenborgh, B. van den Hurk & M. van Aalst (2011). ‘Projected changes in mean and extreme precipitation in Africa under global warming. Part II: East Africa’. In: *Journal of Climate* 24.14, pp. 3718–3733. DOI: 10.1175/2010jcli2883.1.

Stan, K. & A. Sanchez-Azofeifa (2019). ‘Tropical dry forest diversity, climatic response, and resilience in a changing climate’. In: *Forests* 10.5, p. 443. DOI: 10.3390/f10050443.

716 Stern, R. D., M. D. Dennett & D. J. Garbutt (1981). ‘The start of the rains in West Africa’. In:
717 *Journal of Climatology* 1.1, pp. 59–68. DOI: 10.1002/joc.3370010107.

718 Stevens, N., C. E. R. Lehmann, B. P. Murphy & G. Durigan (2016). ‘Savanna woody encroachment
719 is widespread across three continents’. In: *Global Change Biology* 23.1, pp. 235–244. DOI: 10 .
720 1111/gcb.13409.

721 Stöckli, R., T. Rutishauser, I. Baker, M. A. Liniger & A. S. Denning (2011). ‘A global reanalysis of
722 vegetation phenology’. In: *Journal of Geophysical Research* 116.G3. DOI: 10.1029/2010jg001545.

723 Tadross, M. A., B. C. Hewitson & M. T. Usman (2005). ‘The interannual variability of the onset
724 of the maize growing season over South Africa and Zimbabwe’. In: *Journal of Climate* 18.16,
725 pp. 3356–3372. DOI: 10.1175/jcli3423.1.

726 Tilman, D., F. Isbell & J. M. Cowles (2014). ‘Biodiversity and ecosystem functioning’. In: *Annual*
727 *Review of Ecology, Evolution, and Systematics* 45, pp. 471–493. DOI: 10.1146/annurev-ecolsys-
728 120213-091917.

729 Timberlake, J. R. & G. M. Calvert (1993). ‘Preliminary root atlas for Zimbabwe and Zambia’. In:
730 *The Zimbabwe Bulletin of Forestry Research* 10.

731 Velasque, M. & K. Del-Claro (2016). ‘Host plant phenology may determine the abundance of an
732 ecosystem engineering herbivore in a tropical savanna’. In: *Ecological Entomology* 41.4, pp. 421–
733 430. DOI: 10.1111/een.12317.

734 Vinya, R., Y. Malhi, N. D. Brown, J. B. Fisher, T. Brodribb & L. E. O. C. Aragão (2018). ‘Seasonal
735 changes in plant-water relations influence patterns of leaf display in Miombo woodlands: evidence
736 of water conservative strategies’. In: *Tree Physiology* 39.1. Ed. by G. Goldstein, pp. 104–112. DOI:
737 10.1093/treephys/tpy062.

738 Wainwright, C. M., E. Black & R. P. Allan (2021). ‘Future changes in wet and dry season charac-
739 teristics in CMIP5 and CMIP6 simulations’. In: *Journal of Hydrometeorology* 22, pp. 2339–2357.
740 DOI: 10.1175/jhm-d-21-0017.1.

741 Wallis, C. I. B., S. Kothari, J. R. Jantzen, A. L. Crofts, S. St-Jean, D. Inamdar, J. P. Arroyo-Mora,
742 M. Kalacska, A. Bruneau, N. Coops et al. (2024). ‘Exploring the spectral variation hypothesis
743 for α - and β -diversity: A comparison of open vegetation and forests’. In: *Environmental Research*
744 *Letters*. DOI: 10.1088/1748-9326/ad44b1.

745 Warren, J. M., R. J. Norby & S. D. Wullschleger (2011). ‘Elevated CO₂ enhances leaf senescence
746 during extreme drought in a temperate forest’. In: *Tree Physiology* 31.2, pp. 117–130. DOI: 10 .
747 1093/treephys/tpr002.

748 White, F. (1983). *The Vegetation of Africa: A descriptive memoir to accompany the UNESCO /*
749 *AETFAT / UNSO vegetation map of Africa*. Paris, France: UNESCO. DOI: 10.2307/2260340.

750 Whitecross, M. A., E. T. F. Witkowski & S. Archibald (2017). ‘Savanna tree-grass interactions:
 751 A phenological investigation of green-up in relation to water availability over three seasons’. In:
 752 *South African Journal of Botany* 108, pp. 29–40. DOI: 10.1016/j.sajb.2016.09.003.
 753 Whitley, R., J. Beringer, L. B. Hutley, G. Abramowitz, M. G. De Kauwe, B. Evans, V. Haverd,
 754 L. Li, C. Moore, Y. Ryu et al. (2017). ‘Challenges and opportunities in land surface modelling of
 755 savanna ecosystems’. In: *Biogeosciences* 14.20, pp. 4711–4732. DOI: 10.5194/bg-14-4711-2017.
 756 Zani, D., T. W. Crowther, L. Mo, S. S. Renner & C. M. Zohner (2020). ‘Increased growing-season
 757 productivity drives earlier autumn leaf senescence in temperate trees’. In: *Science* 370.6520,
 758 pp. 1066–1071. DOI: 10.1126/science.abd8911.
 759 Zhou, Y., B. J. Wigley, M. F. Case, C. Coetsee & A. C. Staver (2020). ‘Rooting depth as a key woody
 760 functional trait in savannas’. In: *New Phytologist* 227.5, pp. 1350–1361. DOI: 10.1111/nph.16613.
 761 Zuur, A. F., E. N. Ieno & C. S. Elphick (2010). ‘A protocol for data exploration to avoid common
 762 statistical problems’. In: *Methods in Ecology and Evolution* 1, pp. 3–14. DOI: 0.1111/j.2041-
 763 210X.2009.00001.x.

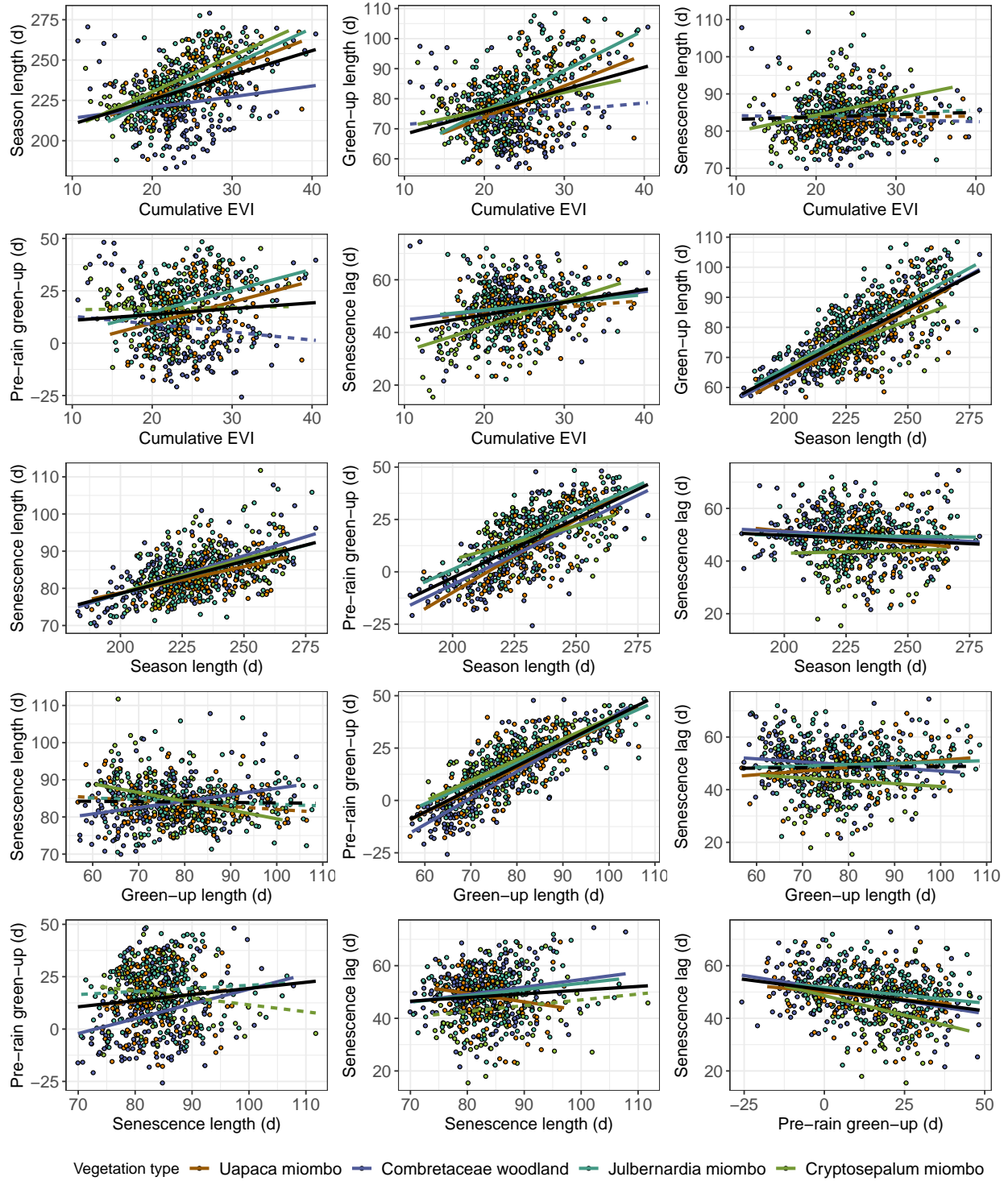


Figure S1: Scatter plots showing pairwise comparisons of the six phenological metrics used in this study, extracted from the MODIS MCD12Q2 product (Friedl et al., 2022). Points represent study sites and are coloured by vegetation type. Linear regression line of best fit for all sites is shown as a black line, while linear regressions are shown for each vegetation type as coloured lines. Non-significant linear regression fits ($p < 0.05$) have dashed lines. Units of ‘d’ are the number of days.

Table S1: Performance of models for each phenological metric, showing standardised parameter estimates (95% confidence interval), and goodness of fit statistics. ΔAIC is the difference in AIC between the full model and a null random effects only model. R^2_m and R^2_c refer to the marginal and conditional R^2 , respectively. ICC is the Intra-Class Correlation statistic, which shows how strongly yearly data within each site are correlated. Parameter estimates are marked by an asterisk where the 95% confidence interval does not overlap zero. Models for different phenological metrics used precipitation and degree days from different relevant periods but these values have been combined into single columns in this table. Green-up length and Senescence length used the pre-green-up period, Senescence length and Senescence lag used the pre-senescence period, Cumulative EVI and Season length used the growing season period.

Response	Intercept	Precipitation	Degree days	Species diversity	Stem diameter	Detarioid abundance	ΔAIC	R^2_m	R^2_c	ICC
Cumulative EVI	24.64(0.858)*	0.77(0.111)*	2.67(0.078)*	0.79(0.386)*	0.03(0.375)	-0.6(0.395)*	3713	0.21	0.72	0.65
Season length	235.04(3.044)*	1.38(0.456)*	7.46(0.325)*	4.67(1.364)*	0.81(1.321)	1.72(1.391)*	1893	0.14	0.63	0.57
Green-up length	76.59(1.517)*	-2.9(0.301)*	-6.59(0.425)*	-0.61(0.673)	0.97(0.647)*	-0.29(0.681)	1111	0.20	0.38	0.23
Senescence length	83.14(1.125)*	0.23(0.234)	-0.93(0.324)*	0.24(0.496)	-0.27(0.475)	0.49(0.5)	38	0.01	0.20	0.19
Pre-rain green-up	11.37(1.72)*	-8.56(0.268)*	-8.67(0.399)*	1.04(0.763)*	2.01(0.737)*	1.02(0.776)*	4410	0.45	0.65	0.35
Senescence lag	49.55(1.796)*	0.3(0.44)	2.43(0.329)*	-0.31(0.81)	-2.31(0.777)*	0.48(0.816)	219	0.03	0.30	0.28